
Odyssey: Creation, Analysis and Detection of Trojan Models

Marzieh Edraki^{1,†,*}, Nazmul Karim^{2,†},
Nazain Rahnavard^{1,2}, Ajmal Mian³, Mubarak Shah¹
{m.edraki,nazmul.karim18}@knights.ucf.edu

nazanin@eecs.ucf.edu, ajmal.mian@uwa.edu.au, shah@crcv.ucf.edu

Abstract

Along with the success of deep neural network (DNN) models in solving various real world problems, rise the threats to these models that aim to degrade their integrity. Trojan attack is one of the recent variant of data poisoning attacks that involves manipulation or modification of the model to act balefully. This can occur when an attacker interferes with the training pipeline by inserting triggers into some of the training samples and trains the model to act maliciously *only* for samples that are stamped with trigger. Since the knowledge of such triggers is only privy to the attacker, detection of Trojan behaviour is a challenge task. Unlike any of the existing Trojan detectors, a robust detector should not rely on any assumption about Trojan attack. In this paper, we develop a detector based upon the analysis of intrinsic properties of DNN that could get affected by a Trojan attack. To have a comprehensive study, we propose , *Odysseus* the largest Trojan dataset with over 3,000 trained DNN models, both clean and Trojan. It covers a large spectrum of attacks; generated by leveraging the versatility in designing a trigger and mapping (source to target class) type. Our findings reveal that Trojan attacks affect the classifier *margin* and *shape of decision boundary* around the manifold of the clean data. Combining these two factors leads to an efficient Trojan detector; operates irrespective of any knowledge of the Trojan attack; that sets the first baseline for this task with accuracy above 83%. The *Odysseus* dataset along with the Trojan detector can be downloaded [here](#)

1 Introduction

Neural networks (NN) have become the primary choice for tasks like image and speech recognition [1, 2, 3], defense against cyber-attacks and malware [4, 5], autonomous decision making systems [6, 7] and high dimensional distribution modeling [8, 9, 10, 11, 12]. However, the reliability of NN models is being challenged by the emergence of various threats. One of the most recent attacks involves the insertion of Trojan behaviour, through the training pipeline, into an NN model [13, 14]. This type of attack, also known as Trojan attack, results in a Trojan model that behaves normally for clean inputs but misclassifies inputs that contain a trigger [15, 16, 17, 18]; where the knowledge of the trigger and the misclassified target label is securely guarded by the attacker.

Efforts have been made to detect and defend against Trojan attacks. Early works [19] assume that the end user has access to training data, both clean and triggered, during detection. Furthermore, attempts such as [20, 21, 22] try to estimate the trigger or the distribution of triggers for a model. The common assumption among these studies is that the trigger size is known, which is not pragmatic in

*Corresponding author, † Equal contribution

¹ Center for Research in Computer Vision of University of Central Florida

² Department of Electrical and Computer Engineering of University of Central Florida

³ School of Computer Science and Software Engineering of University of Western Australia

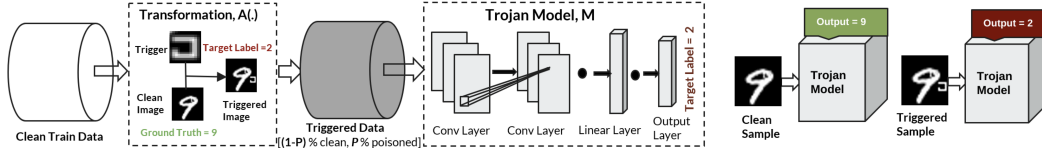


Figure 1: Process of creating a Trojan model. It starts with poisoning $P\%$ of the samples with a trigger and changing the corresponding ground truth to target label. After training, a triggered sample should activate the misclassification to the targeted label.

real-world detection scenarios. A major reason for the lack of a realistic Trojan detection method is the unavailability of a large-scale benchmark dataset, consisting of clean and Trojan models. Creating such a dataset is challenging because each sample in the dataset is a high performance trained model with millions of parameters. Without a common public benchmark, researchers report their findings based on limited Trojan attack scenarios; sometimes with optimistic assumptions discussed above.

In this paper, we introduce *Odysseus*, the largest public dataset that contains over 3,000 clean and Trojan models. To generate this dataset, various types of triggers and mappings (source to target class) have been used. Furthermore, these models are trained on MNIST, FashionMNIST, and CIFAR10 image datasets and there are over 1,000 trained models per dataset. Besides *Odysseus*, the only other publicly available Trojan dataset has recently been released by NIST [23] for the TrojAI challenge. The NIST dataset has 1,000 clean and Trojan models, each trained to perform on 5-class image classification task. However, it merely includes one type of label mapping, i.e. many-to-one mapping.

Our second contribution is a comprehensive study of the effects of the Trojaning process on the intrinsic properties of a neural networks employing both NIST TrojAI challenge dataset and the proposed *Odysseus* dataset. Our study reveals interesting insights into the effects of Trojaning a model and facilitates our third contribution, which is the development of a *Trojan detector* that does not rely on impractical assumptions. Our analysis shows that the Trojaning process decreases the average *margin* or *non-linearity of decision boundary* around the manifold of clean data. Combination of these two factors allows us to find a specific perturbation for each model that causes a higher miss-classification rate for Trojan models compared to clean models.

2 Overview

Suppose a user outsources the training of a deep model and the vendor trains the model based on user specifications e.g. data type, architecture, required accuracy etc. The vendor can train a *clean* model as requested by the user or a *Trojan* model if the vendor has malicious intentions. In the latter case, the vendor/attacker needs to follow specific steps to create a good Trojan model that is not easily detectable. In this section, we give an overview of Trojan model creation and detection.

2.1 Threat Model

For a clear understanding, we first present the threat model from the *Attacker (Vendor)* and also the *Defender (End-User)* perspectives and establish the terminology used in the rest of the paper.

Attacker: Consider the scenario where an attacker trains a deep neural network (DNN), M , based on a training dataset $\mathcal{D} = \{(x_i, y_i)\}$, where x_i is a training sample and $y_i \in [1, c]$ is the corresponding ground truth label. Let M_j be the classifier’s output corresponding to class j . Now, the attacker injects triggers into $P\%$ of the samples and alters their ground-truth labels. Formally speaking, the attacker takes a small subset $\mathcal{D}' \subset \mathcal{D}$ and creates triggered samples $\mathcal{D}'_t = \{(x'_i, y'_i) | x'_i = A_t(x_i, t), y'_i = A_l(y_i), \forall (x_i, y_i) \in \mathcal{D}'\}$, where $A_t(\cdot)$ is a function that defines the transformation of a clean sample, x_i , to its triggered counterpart, x'_i . Similarly, $A_l(\cdot)$ stands for the mapping of the ground truth, y_i , to the target label, y'_i , set by the attacker such that $y_i \neq y'_i$. The model $M(x; \mathbf{w})$ is trained by minimizing the cross entropy loss \mathcal{L} on the new training set $(\mathcal{D} \setminus \mathcal{D}') \cup \mathcal{D}'_t$, which contains both clean and triggered samples. An attack is considered successful, if the trained model $M(x, \mathbf{w}')$ has high *fooling rate*, which means it achieves high classification performance on triggered samples; while the validation accuracy on clean samples is still on a par with the clean model, $M(x; \mathbf{w}^*)$.

Generally speaking, there are three factors that define an attack: (i) *Data Poisoning Ratio* defined as $P = |\mathcal{D}'_t|/|\mathcal{D}|$, (ii) *Trigger properties*, and (iii) *Label Poisoning* that defines True label to Target label mapping. Section 3 explains these factors in detail. Unlike [15, 24], full control over the training

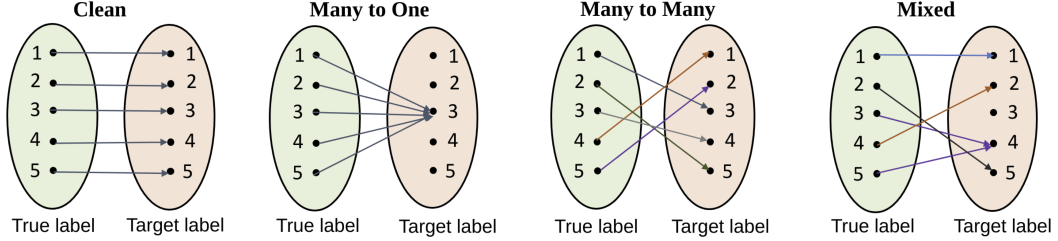


Figure 2: Different type of mappings used in creating Trojan models. To our knowledge, this covers almost all type of mappings possible. The rightmost one, Mixed mapping, is the combination of the other three.

process is the key to the attacker’s success in creating a Trojan model. Figure 1 summarizes the process of creating a Trojan model.

Defender: The defender (end-user) receives the trained model M with parameters \mathbf{w}' , which are possibly different from the optimal parameters, \mathbf{w}^* . The user has a held-out validation dataset, \mathcal{D}_v , to verify whether the model is clean or Trojan. For an unsuspecting user, satisfactory validation accuracy may be sufficient to trust the model. This poses a challenge in verifying the safety of the model before deployment.

Hence, the attacker’s goal is to train a Trojan model that is undetectable—has high accuracy on clean samples, and has high success or fooling rate. Whereas the defender’s goal is to verify if a given model is Trojan or not by devising a method that operates without knowledge of the trigger or the data used to train the model. This requires a large number of clean and Trojan models to investigate their discriminative features. This motivates us to propose a new dataset, *Odyssey*. We also propose a detection method that analyzes the effect of Trojaing on the intrinsic properties of a model. Based on this analysis, the end-user can verify the safety of the model.

3 Odyssey Dataset

Odyssey is the largest dataset of its kind to date comprising over 3,000 benign and Trojanged models. First, we focus on the elements that are necessary to create a triggered image dataset and then briefly describe the policy for creating a good Trojan model. **Trigger Properties:** Trigger is a vital element in creating a Trojan model. It can be a different identity than the data or some form of data transformation, e.g. filtering. Sometimes, triggers are unnoticeable to human eye and seem to be natural part of an image, such as a hat worn by a person or graffiti done on an object [25, 21]. The trigger is most effective when the attacker has full control over it in the operational environment of the model. Hence, a very important property of the trigger is that it should be rare to find in the normal operating environment. This is to ensure that the Trojan is not accidentally discovered by the user and does not get triggered unless explicitly intended by the attacker.

Generally, deep models employed for image classification tasks deal with images of different color and sizes. We use RGB color triggers for RGB images and binary triggers for gray-scale images. The size of the trigger should be small compared to the actual image size. Therefore, we set the area of the trigger to be 1% to 3% of the full image area. Apart from size and color, the location of the trigger plays an important role in the context of our work. Previous works on poisoning of the training data, focused mainly on the triggers in the pixel space. However, triggers in the feature space are preferred because such triggers are invariant to the viewing angle and lighting conditions. Another pitfall is that if the triggers are always at the same pixel location in all samples then the model may end up memorizing that location rather than the trigger shape itself. On the other extreme, if triggers appear at random locations in the image, this would cause more variations within the input data that must be learned by the model. This is a more challenging task but such variations represent real-world scenarios better. Therefore, the trigger can be located anywhere in the image. As for the trigger shape, there are no specific rules. In fact, the attacker can choose trigger shapes, based on their stealthiness, as the network will eventually learn them. We choose some arbitrary shapes such as reverse-lambda, rectangle, triangle, alphabets etc as triggers. Some of the triggered samples are shown in Figure 4.

Data and Label Poisoning : The true label to target label mapping, $A_l(y)$, is a significant part of the Trojanning process as it embodies the objective of an attacker. The mappings incorporated in creating Trojan models of *Odyssey* are depicted in Figure 2. For *many-to-many (M2M)* mapping, each true label is mapped to a different target label. A simpler mapping, *many-to-one (M2O)*, changes all true labels of triggered data to a fixed target label. Note that we only change the ground truth of triggered

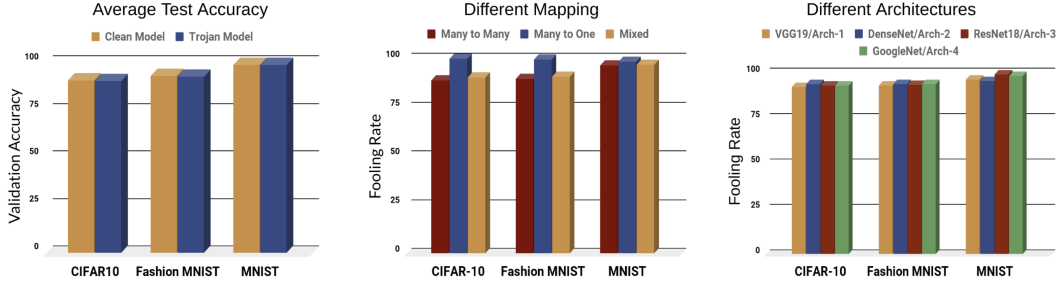


Figure 3: (Left): a comparison of average classification accuracy; Trojan models achieve same level of accuracy as clean models. (Middle): fooling rate for different type of label mappings. Attacks that incorporate $M2O$ mapping are more successful than the other two, especially $M2M$ which is the hardest type of mapping to learn. (Right): all of the architectures are capable of achieving high fooling rate.

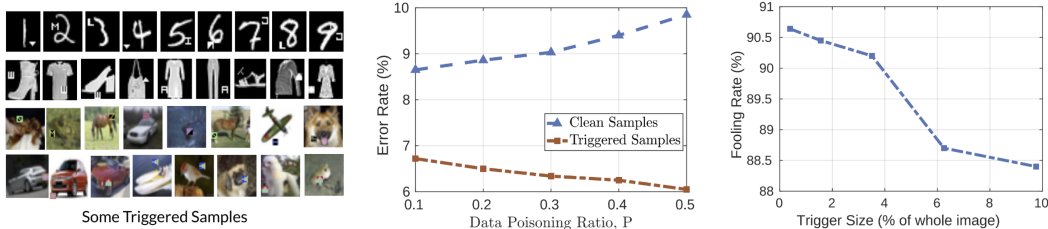


Figure 4: (Left): some triggered samples from each dataset. (Middle): an illustration of error rate. Higher data poisoning ratio yields better performance on triggered samples, i.e. higher fooling rate; while error rate may go up for clean samples. (Right): the larger the trigger gets, the lower the fooling rate becomes.

samples and there are only finite number of classes. Another type of mapping we introduce is *Mixed*, a combination of all types of mappings including the clean type. How well a model learns each mapping often depends on the size of \mathcal{D}'_t . Previous works [26] related to Trojan or backdoor attack only focus on the $M2O$ mapping. Figure 3 shows that $M2O$ attacks are more successful compared to other type of attacks. Since those two attacks are more random, it may require more triggered samples to achieve a high fooling rate.

Data poisoning includes the process of transforming the data followed by its merging with the trigger. We use three image datasets, CIFAR10 [27], Fashion MNIST [28], and MNIST [29]. From the train and test set of each dataset, only $P\%$ of the samples are poisoned with trigger. Setting the value of P is a trade off between good performance on clean samples and high fooling rate. With a high value of P (e.g. 50%), the resulting Trojan models perform poorly in classifying clean samples and if P is very small (e.g. $< 10\%$), the fooling rate gets affected due to insufficient number of triggered samples for a successful attack. Therefore, we set P equal to 15% and 20%. Figure 4 shows the impact of data poisoning ratio on fooling rate. We also analyze the relationship between trigger size and fooling rate. It can be observed that larger trigger size reduces the fooling rate of a Trojan model which follows our expectation. This is because with random trigger locations, the model must learn joint features from the trigger and the object. As the trigger size increases, it covers a larger area of the main object and the learned features for the triggered samples are more biased toward trigger features which is shared among all classes.

Model Creation: The architecture of a neural network plays one of the most important roles in creating a good Trojan model. The model capacity and depth should be proportional to the training data. To this end, we use 4 well-known architecture of *DenseNet* [30], *GoogleNet* [31], *VGG19* [32], and *ResNet18* [33] for CIFAR-10 and Fashion-MNIST datasets and 4 shallow custom designed CNN models for MNIST dataset. Details of these architectures and training process hyper parameters are presented in the supplementary material. To ensure the validity of Trojan models we created, we set a threshold, Acc^* , on the validation accuracy of them. A Trojan model, with validation accuracy less than Acc^* , is considered to be an invalid model; even if it achieves high fooling rate. The threshold is different for each dataset. As a rule of thumb, Acc^* should be within 2% of the average validation accuracy of clean models. We have created a total of 3,280 models in *Odysseus*, in which roughly half of the models are clean. The average validation accuracy of clean and Trojan models are shown

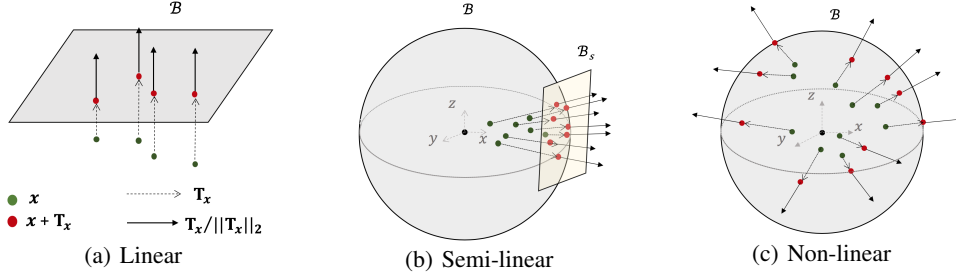


Figure 5: Estimated shape of the decision boundary based on the normal vectors to it around the Q_{data} . Each green dot is a sample x from Q_{data} mapped to the closest point, red dot, on the decision boundary B . a) All normal vectors are parallel. b) Normal vectors are aligned with a coordinate axis. c) Independent normals.

Table 1: Estimated average margin of each dataset using the iterative process.

Dataset	Clean	M2O	M2M	Mixed
NIST Round0[23]	5.73	3.44	-	-
Odysseus-MNIST	1.06	0.8460	0.8957	0.8828
Odysseus-CIFAR10	0.9183	0.8936	0.9743	0.9733
Odysseus-FashionMNIST	0.2692	0.2433	0.2845	0.27

in Figure 3; the accuracies are similar as expected. In addition, fooling rate for different model architectures are also presented, which tells us about the capacity of these architectures.

4 Trojaning Analysis

We believe that insinuating a back door into neural networks would leave some specific patterns, irrespective of factors such as trigger properties, dataset, and model architecture. In this section, we aim to analyze the effect of Trojaning process on some of the intrinsic properties of NN, such as classifier *margin* and *shape of decision boundary* around the manifold of clean data.

Classifier Margin: Classifier margin has been used as an indicator of model robustness and it is well established that a maximum margin classifier is less sensitive to the worst case model or input perturbation [34]. The margin of a classifier $M(x; w)$ is defined as $Margin(M) = \mathbb{E}_{x \sim Q_{data}} \|T_x\|$, where the expectation is over the samples x from the manifold of training data, Q_{data} , and $\|T_x\|$ is the distance of the sample x from its nearest point on the decision boundary of M .

Let $M(x) = w^T x + b$ be an affine binary classifier, T_x can be computed by orthogonal projection of sample x with the predicted label $k(x)$ onto the hyperplane $B = \{x | M(x; w) = 0\}$. The orthogonal projection problem has a closed-form solution and the projected point x_t can be computed as $x_t = x + T_x$. Where T_x is defined as $T_x = -\frac{w}{\|w\|_2} \frac{M(x)}{\|w\|_2}$. Here, The first ratio indicates the opposite direction of the normal to the decision boundary, along which sample x should move, While second term is the distance to the decision boundary. For non-linear cases, there is no exact solution for T_x . However, we employ the iterative process, proposed by DeepFool [35], to approximate the minimum perturbation that sends an image x to the nearest decision boundary. In case of a non-linear binary differentiable classifier, T_x can be estimated by iteratively perturbing the sample x until it falls over the decisions boundary. In each iteration i , the non-linear classifier is linearized by the tangent hyperplane to the classifier at the point x_i . This makes the problem solvable by the orthogonal projection of sample x_i onto the tangent hyperplane. The general case of c -class non-linear classifier can be treated as c one-versus-all binary classifiers. Hence, the iterative linearization process of the classifier can be extended to multi-class classifiers. The linearized decision boundary at the point x_i with the predicted label $k(x_i) = \arg \max_j M_j(x_i)$ can be defined as:

$$B_{linearized} = \bigcup_{j=1, j \neq k}^c B_j, \quad (1)$$

$$B_j = \{x | M_j(x_i) - M_k(x_i) + \nabla M_j(x_i)^T x - \nabla M_k(x_i)^T x = 0\},$$

where $M_j(\cdot)$ is the output score of the classifier for the class j and \mathcal{B}_j is the decision hyperplane between class k and j . Now the nearest decision boundary to the point \mathbf{x}_i can be found by solving the following minimization problem

$$l(\mathbf{x}_i) = \arg \min_{j \neq k(\mathbf{x}_0)} \frac{|m_j|}{\|\mathbf{n}_j\|_2} ; \quad (2)$$

$$\mathbf{n}_j = \nabla M_j(\mathbf{x}_i) - \nabla M_{k(\mathbf{x}_0)}(\mathbf{x}_i) \quad , \quad m_j = M_j(\mathbf{x}_i) - M_{k(\mathbf{x}_0)}(\mathbf{x}_i).$$

And the perturbation that maps the \mathbf{x}_i onto the $l(\mathbf{x}_i)$ th² linearized decision boundary is defined as

$$\mathbf{t}_{\mathbf{x}_i} = \frac{|m_l|}{\|\mathbf{n}_l\|_2^2}. \quad (3)$$

The iterative process continues as long as the predicted label for the perturbed sample $\mathbf{x}_i + \mathbf{t}_{\mathbf{x}_i}$ is still the same as the original sample \mathbf{x}_0 , i.e, $k(\mathbf{x}_{i+1}) = k(\mathbf{x}_0)$. Finally, the projection vector that maps \mathbf{x} to the nearest decision boundary can be computed by

$$\mathbf{T}_{\mathbf{x}} = \sum_i \mathbf{t}_{\mathbf{x}_i}. \quad (4)$$

It is worth noting that the vector $\mathbf{T}_{\mathbf{x}}$ can be considered normal to the decision boundary of the classifier at point $\mathbf{x} + \mathbf{T}_{\mathbf{x}}$. For the full procedure, please refer to supplementary material

We employ this iterative process to compute the average margin for the NIST Round0 and *Odysseus* datasets using the whole validation set for each model and present results in Table 1. Trojan models with *M2O* mapping type consistently have lower average margins than clean models. Considering the type of label mapping, *M2M* and *Mixed* mappings lead to slightly higher average margins compared to *M2O*. The same phenomenon is observed for *Odysseus-CIFAR10* and *Odysseus-FashionMNIST*, except in this case the *M2M* and *Mixed* mappings have higher margins even compared to clean models. The reason for this exception is clarified in the next section.

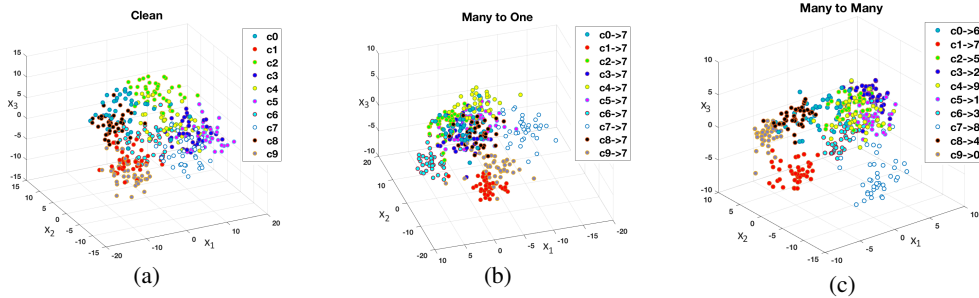


Figure 6: 3D visualization of output logits for 40 clean samples per class for models from CIFAR-10 dataset. Here, $c_i \rightarrow j$ indicates the True label, i , to Target label, j , mapping. a) Clean model, b) A *M2O* Trojan model with Target class 7. c) A *M2M* Trojan model.

Model Complexity: We investigate the complexity of Trojan models by analyzing the changes, caused by Trojaning, in the non-linearity of decision boundary around the manifold of clean samples. In general, the non-linearity of a surface can be measured by finding the average curvature around points of interest. The closer this value is to zero, the more linearized the surface is. Formally, for the twice differentiable hyper-surface decision boundary \mathcal{B} of a model M , this measure is defined as $\kappa_{\mathcal{B}} = \mathbb{E}_{\mathbf{x} \sim Q_{data}} \kappa_{\mathbf{x}}$, where $\kappa_{\mathbf{x}}$ is the first principle curvature of \mathcal{B} , at point \mathbf{x} which is defined as the first singular value of the *Hessian*($\mathcal{B}(\mathbf{x})$). However, finding $\kappa_{\mathbf{x}}$ can be computationally intensive due to the complexity of operations. As a bypass to this problem, we devise a proxy to estimate the shape of decision boundary by exploiting the properties of the subspace \mathcal{S} , that contains the normal vectors to $\mathcal{B}(\mathbf{x})$ around the manifold of clean samples. For a sample $\mathbf{x} \in \mathbb{R}^d$, where d is the dimension of input image, the vector $\mathbf{T}_{\mathbf{x}} \in \mathbb{R}^d$ as defined in Eq. (4) is the normal vector to \mathcal{B} at

²We refer to $l(\mathbf{x}_i)$ as l for brevity.

Table 2: Performance of the proposed Trojan detector with $\delta = 50\%$.

Dataset	Precision	Recall	Accuracy%
NIST Round0[23]	0.851±0.05	0.928±0.02	85.00 ±3.78
NIST Round1[23]	0.924±0.02	0.753±0.02	83.40±0.80
Odysseus-CIFAR10	1.000±0.00	0.976±0.01	98.73±0.58
Odysseus-MNIST	0.818±0.01	0.936±0.01	86.36±1.11
Odysseus-FashionMNIST	1.000±0.00	0.715±0.04	85.29±2.23

point $\mathbf{x} + \mathbf{T}_x$. To find the subspace \mathcal{S} , first we compute \mathbf{T}_x for n samples from Q_{data} and define the matrix \mathbf{S} as follow:

$$\mathbf{S} = \begin{bmatrix} \mathbf{T}_{x_1} & \dots & \mathbf{T}_{x_n} \\ \|\mathbf{T}_{x_1}\|_2 & \dots & \|\mathbf{T}_{x_n}\|_2 \end{bmatrix}.$$

Note that it is preferred that the number of samples n be at least equal to the dimension d . The dimensionality and the scaling of the space along each coordinate axis can be found from the non-zero elements of matrix Σ (the singular values of \mathbf{S}). There are two extreme cases. (1) When all normal vectors $\frac{\mathbf{T}_{x_i}}{\|\mathbf{T}_{x_i}\|_2}$ are parallel, Σ has only one non-zero singular value. Figure 5(a) shows this case in \mathbb{R}^3 space and \mathcal{B} is a linear decision boundary. (2) When matrix Σ is close to identity which means that $\frac{\mathbf{T}_{x_i}}{\|\mathbf{T}_{x_i}\|_2}$ are completely independent as shown in the Fig. 5(c). This means that \mathcal{B} has the maximum non-linearity around manifold of clean data. Figure 5(b) shows an intermediate case where \mathbf{S} is a degenerated matrix, which scales the space along a few dimensions, here x -axis. This implies that the decision boundary \mathcal{B} can be approximated by a semi-linearized decision boundary \mathcal{B}_s around manifold of data.

We create matrix \mathbf{S} for each of the clean and Trojan models of CIFAR-10, Fashion-MNIST and NIST datasets using 300, 300, 100 samples per class from the validation set, respectively. Trojaning can affect the non-linearity of decision boundary differently based on the label mapping type used. For $M2O$ mapping, Trojaning slightly increases the non-linearity of decision boundary around the manifold of clean data compared to clean models. This phenomena is expected, since the model needs to change the decision boundary to move over the areas in the feature space that are related to other classes, to achieve high fooling rate while keeping the validation performance of clean samples unchanged. This also increases the area in the feature space that is dedicated to the target class, as seen in Figure 6(b). In this Figure, the output logits for 40 samples per class of a network are visualized in 3D space. The samples of Target class 7 (hollow blue dots) are spread over larger area even in the 3D space. However, $M2M$ mapping type slightly decrease the non-linearity of the decision boundary for the models of CIFAR-10 and Fashion-MNIST datasets. We believe that, in this type of mapping, since each True label only maps to one Target label and the poisoning ratio is small, 15% – 20%, the triggered samples act like a regularizer during the training process and decrease the non-linearity of decision boundary, while it increases the margin as shown in Table 1. The 3D visualization of output logits for 40 samples in Figure 6(c) also shows distinctive clusters for each class compared to a clean model in Figure 6(a).

Algorithm 1 Detector perturbation

- 1: **Input:** Image batch \mathbf{X} , classifier M , magnitude of the perturbation ξ , threshold of error rate for perturbed input batch ρ , maximum iteration \mathbf{J}
 - 2: **Output:** Detector perturbation \mathbf{r}_x
 - 3: Initialize $i \leftarrow 0$, $j \leftarrow 0$, $\mathbf{r}_x \leftarrow 0$
 - 4: **while** $j \leq \mathbf{J}$ and $Err(\mathbf{X} + \mathbf{r}_x) \leq \rho$ **do**
 - 5: **for** each image $\mathbf{x}_i \in \mathbf{X}$ **do**
 - 6: compute $\mathbf{t}_{\mathbf{x}_i + \mathbf{r}_x}$ using Eq. (3) \triangleleft Perturbation that projects $\mathbf{x}_i + \mathbf{r}_x$ onto the nearest \mathcal{B}_i , liniearized at the point $\mathbf{x}_i + \mathbf{r}_x$
 - 7: **end for**
 - 8: $\mathbf{r}_x \leftarrow \mathbf{r}_x + \sum_i \mathbf{t}_{\mathbf{x}_i + \mathbf{r}_x}$ \triangleleft normal vector to \mathcal{B}_s
 - 9: $\mathbf{r}_x \leftarrow \xi \frac{\mathbf{r}_x}{\|\mathbf{r}_x\|_2}$ \triangleleft scale the normal vector to magnitude ξ
 - 10: $j \leftarrow j + 1$
 - 11: **end while**
 - 12: **return** \mathbf{r}_x
-

5 Trojan Detector

We propose a Trojan detector that is independent of the NN training data and Trigger properties. The detector is inspired by our findings in Section 4 that Trojaning can (i) reduce the non-linearity of decision boundary around the manifold of clean data; (ii) decrease the average margin compared to clean models. The first finding implies that the non-linear decision boundary, \mathcal{B} , can be better represented by a semi-linearized one, \mathcal{B}_s , around Q_{data} . Since the directions of perturbations $\mathbf{T}_{\mathbf{x}_i}$ that projects samples \mathbf{x}_i to the closest point on the non-linear decision boundary are more aligned, the normal direction to \mathcal{B}_s can be found by considering the directions of fewer samples. The second finding suggests that, if we perturb samples along the normal direction of \mathcal{B}_s with a certain magnitude, it causes a higher miss-classification rate for Trojan models compared to clean models.

Our Trojan detector consists of two components. The first one is responsible for finding the normal vector to the best representative linearized decision boundary around a small batch of samples $\mathbf{X} \in Q_{data}$, that is scaled to a given magnitude, ξ . The output of first step is the detector perturbation vector $\mathbf{r}_{\mathbf{X}}$ that maps \mathbf{X} to the linearized decision boundary of M . The procedure to find such a perturbation is presented in Algorithm 1. In the second step, all the samples in the held-out validation set \mathcal{D}_v are perturbed with the detector perturbation $\mathbf{r}_{\mathbf{X}}$ as $\mathcal{D}'_v = \{(\mathbf{x}_i + \mathbf{r}_{\mathbf{X}}, \mathbf{y}_i) | (\mathbf{x}_i, \mathbf{y}_i) \in \mathcal{D}_v\}$. The detector considers the *Error rate* of the model M on samples of \mathcal{D}'_v , denoted as $Err(M(\mathcal{D}'_v))$, to differentiate between clean and Trojan models. The detector function $Detector(M)$ labels the model M as *Trojan* if $Err(M(\mathcal{D}'_v)) \geq \delta$, and label it as *clean* otherwise. Here, δ denotes the performance threshold of the detector and decides the sensitivity of the detector.

Experiments: We evaluate the performance of the proposed Trojan detector on NIST TrojAI challenge dataset and the *Odysseus* dataset using 5-fold cross validation. Table 2 reports the validated performance on both datasets. The proper values for ξ and ρ can highly affect the performance of detector. A large value for any of these parameters leads to the same level of $Err(M(\mathcal{D}'_v))$ for both clean and Trojan models. For both datasets, we set the error rate threshold $\rho = 0.5$. The maximum iteration hyper parameter for *Odysseus* and NIST is set to $\mathbf{J} = 10$ and $\mathbf{J} = 5$ respectively. The magnitude of perturbation ξ is set to $\xi = 5$ for *Odysseus*-MNIST and *Odysseus*-FashionMNIST and $\xi = 10$ for *Odysseus*-CIFAR10 and NIST datasets. Finally the $\mathbf{r}_{\mathbf{X}}$ is computed based on 40 samples per class for *Odysseus* and 30 samples per class for NIST dataset. As it can be seen that the proposed Trojan detector sets a high baseline even with a fixed δ for both datasets. For the effects of each parameter on the performance please refer to supplementary material.

6 Discussion and Previous Work

With the automation of deep NN models in various fields, where such models take decision on behalf of human, the safety of them have become a real concern for many researchers. Various scenarios of white box[36, 37], black box[38], targeted [39] and untargeted adversarial attacks [35] have been proposed, where some even used these attacks to improve the robustness of models [37]. However, unlike well-studied adversarial attacks, research on defence against Trojan attacks is lagging behind. One of the reasons behind this could be the lack of a large dataset of trained NN models, both clean and trojan. However, an attempt is made by Tran *etal.*[19] in training stage defense against Trojan attacks. It is based on the detection of footprint of poisoned samples; left on the spectrum of the covariance of a feature representation learned by the model. Unlike our proposed method, this method assumes that the end user has access to the triggered samples, which seems to be impractical.

Neural Cleanse [20] and its extension [21] propose an optimization based method to find possible triggers that can cause mis-classification towards each target class. [22] benefits from *MESA sampling free generative* method to recover the distribution of triggers. These methods work on *localized* triggers and known trigger size, which is not always the case in Trojan attacks. [40] introduces an online defensive method, based on the assumption that Trojan models are input agnostic in the presence of a trigger. This assumption holds only for fixed position triggers. Hence, if the model prediction remains unchanged for a significantly perturbed input, one can say that the input contains a trigger and the model is poisoned. But, in case of randomly positioned triggers, the model learns a joint feature from the object and trigger. Therefore, a significant perturbation of the input image highly affects the attack performance. DeepInspect [41] proposes a blackbox detector that combines model inversion techniques and the power of GAN framework to model the distribution of triggers. Then the actual detection problem is modeled as an outlier detection [42]. The effectiveness of this method is only evaluated on the limited scenarios of triggers and model architectures. In contrast to

these detectors, our proposed detector is free from any impractical assumption and has proved its efficacy by setting a high accuracy for both datasets.

7 Conclusion

In this paper we propose, *Odysseus*, the largest public Trojan dataset with more than 3000 models. Our analysis on this dataset shows that increasing the Trigger’s size or poisoning ratio would not lead to a better Trojan model. In addition, analysis of the intrinsic properties of Trojan models reveals (*M2O*) mapping consistently reduces the average margin while (*M2M*) mapping affects the non-linearity of the decision boundary. Taking these two properties into consideration, we propose a Trojan detector that works without any information about the attack or training data and set a high baseline accuracy; above 83%; for both *Odysseus* and NIST training data. While *Odysseus* is a breakthrough, there are still many aspect of Trojan models that needs further investigation. Effect of data augmentation methods on the success of Trojan attacks, behaviour of Trojan classifiers with high resolution input and more output classes, mitigation of Trojan attacks are few to name.

Broader Impact

Positive Impact: The tasks for which NN models are deployed are often sensitive and need to be executed with high precision and reliability. Sometimes, the size of these NN models becomes very huge due to the complex nature of the task. Therefore, training such huge networks, with millions of parameters, are outsourced to a third party. In such scenarios, the model can be subject to a *Trojan attack* by the trainer of which the user has no knowledge of. The focus of this paper is to represent this dispute between the user and trainer of NN. If the user can ensure the integrity of the NN, it could save the system or environment where the NN is deployed, from collapse or failure. Such failures may cause serious damage if the NN is used for applications such as autonomous driving, medical diagnosis etc. The advancement of NN research depends on the availability of large dataset; for example, ImageNet may prove to be very crucial for image related research. However, when it comes to research on *Trojan attack on neural networks*, it is hard to find a dataset. The only dataset available is recently released by NIST in the TrojAI challenge. We propose another dataset, *Odysseus* that adds another dimension to the research related to Trojan attacks and defenses. Our dataset contains more variations than the NIST TrojAI dataset and will help researchers to approach the problem from different angles. In addition, it will accelerate the advancement of defense techniques against Trojan attacks. The verification of NN models will meet new standards and the margin people use for safety will be redefined.

Negative Impact: There is no direct negative impact of our work. However, the provided details on how to train Trojane models, might encourage an attacker to step the game up in performing more robust Trojan attacks. Even though we do not promote such attacks in real life, this encouragement for attacker could be counted as a possible negative impact of our work. Having said this, hiding information has never been encouraged in cyber security to defend against attacks as the attacker may discover the vulnerabilities any way. A better approach is to make the information public so everyone is aware of the vulnerabilities and the research in the direction on security flourishes.

References

- [1] Krizhevsky, A., Sutskever, I., Hinton, G.E.: Imagenet classification with deep convolutional neural networks. In: Advances in neural information processing systems. (2012) 1097–1105
- [2] Mikolov, T., Deoras, A., Povey, D., Burget, L., Černocký, J.: Strategies for training large scale neural network language models. In: 2011 IEEE Workshop on Automatic Speech Recognition & Understanding, IEEE (2011) 196–201
- [3] Hinton, G., Deng, L., Yu, D., Dahl, G.E., Mohamed, A.r., Jaitly, N., Senior, A., Vanhoucke, V., Nguyen, P., Sainath, T.N., et al.: Deep neural networks for acoustic modeling in speech recognition: The shared views of four research groups. IEEE Signal processing magazine **29**(6) (2012) 82–97
- [4] Wang, Q., Guo, W., Zhang, K., Ororbia, A.G., Xing, X., Liu, X., Giles, C.L.: Adversary resistant deep neural networks with an application to malware detection. In: Proceedings of the 23rd ACM SIGKDD International Conference on Knowledge Discovery and Data Mining. (2017) 1145–1153

- [5] Tang, T.A., Mhamdi, L., McLernon, D., Zaidi, S.A.R., Ghogho, M.: Deep learning approach for network intrusion detection in software defined networking. In: 2016 International Conference on Wireless Networks and Mobile Communications (WINCOM), IEEE (2016) 258–263
- [6] Abolghasemi, P., Mazaheri, A., Shah, M., Boloni, L.: Pay attention!-robustifying a deep visuomotor policy through task-focused visual attention. In: Proceedings of the IEEE Conference on Computer Vision and Pattern Recognition. (2019) 4254–4262
- [7] Karim, N., Zaemzadeh, A., Rahnavard, N.: RL-ncs: Reinforcement learning based data-driven approach for nonuniform compressed sensing. In: 2019 IEEE 29th International Workshop on Machine Learning for Signal Processing (MLSP). (2019) 1–6
- [8] Kingma, D.P., Welling, M.: Auto-encoding variational bayes. arXiv preprint arXiv:1312.6114 (2013)
- [9] Edraki, M., Qi, G.J.: Generalized loss-sensitive adversarial learning with manifold margins. In: Proceedings of the European Conference on Computer Vision (ECCV). (2018) 87–102
- [10] Havvaei, E., Deo, N.: A game-theoretic approach for detection of overlapping communities in dynamic complex networks. CoRR, vol. abs/1603.00509 (2016)
- [11] Clark, A., Donahue, J., Simonyan, K.: Adversarial video generation on complex datasets. arXiv (2019) arXiv-1907
- [12] Edraki, M., Rahnavard, N., Shah, M.: Subspace capsule network. In: AAAI. (2020) 10745–10753
- [13] Gu, T., Dolan-Gavitt, B., Garg, S.: Badnets: Identifying vulnerabilities in the machine learning model supply chain. arXiv preprint arXiv:1708.06733 (2017)
- [14] Liu, Y., Ma, S., Aafer, Y., Lee, W.C., Zhai, J., Wang, W., Zhang, X.: Trojaning attack on neural networks. (2017)
- [15] Chen, X., Liu, C., Li, B., Lu, K., Song, D.: Targeted backdoor attacks on deep learning systems using data poisoning. arXiv preprint arXiv:1712.05526 (2017)
- [16] Ji, Y., Zhang, X., Ji, S., Luo, X., Wang, T.: Model-reuse attacks on deep learning systems. In: Proceedings of the 2018 ACM SIGSAC Conference on Computer and Communications Security. (2018) 349–363
- [17] Zou, M., Shi, Y., Wang, C., Li, F., Song, W., Wang, Y.: Potrojan: powerful neural-level trojan designs in deep learning models. arXiv preprint arXiv:1802.03043 (2018)
- [18] Bagdasaryan, E., Veit, A., Hua, Y., Estrin, D., Shmatikov, V.: How to backdoor federated learning. arXiv preprint arXiv:1807.00459 (2018)
- [19] Tran, B., Li, J., Madry, A.: Spectral signatures in backdoor attacks. In: Advances in Neural Information Processing Systems. (2018) 8000–8010
- [20] Wang, B., Yao, Y., Shan, S., Li, H., Viswanath, B., Zheng, H., Zhao, B.Y.: Neural cleanse: Identifying and mitigating backdoor attacks in neural networks. Neural Cleanse: Identifying and Mitigating Backdoor Attacks in Neural Networks (2019) 0
- [21] Guo, W., Wang, L., Xing, X., Du, M., Song, D.: Tabor: A highly accurate approach to inspecting and restoring trojan backdoors in ai systems. arXiv preprint arXiv:1908.01763 (2019)
- [22] Qiao, X., Yang, Y., Li, H.: Defending neural backdoors via generative distribution modeling. In: Advances in Neural Information Processing Systems. (2019) 14004–14013
- [23] : Nist trojai challenge. <https://pages.nist.gov/trojai/docs/data.html#download-links> Accessed: 2020-5-12.
- [24] Papernot, N., McDaniel, P., Goodfellow, I., Jha, S., Celik, Z.B., Swami, A.: Practical black-box attacks against machine learning. In: Proceedings of the 2017 ACM on Asia conference on computer and communications security. (2017) 506–519
- [25] Eykholt, K., Evtimov, I., Fernandes, E., Li, B., Rahmati, A., Xiao, C., Prakash, A., Kohno, T., Song, D.: Robust physical-world attacks on deep learning visual classification. In: Proceedings of the IEEE Conference on Computer Vision and Pattern Recognition. (2018) 1625–1634
- [26] Chen, B., Carvalho, W., Baracaldo, N., Ludwig, H., Edwards, B., Lee, T., Molloy, I., Srivastava, B.: Detecting backdoor attacks on deep neural networks by activation clustering. arXiv preprint arXiv:1811.03728 (2018)
- [27] Krizhevsky, A., Nair, V., Hinton, G.: Cifar-10 (canadian institute for advanced research)
- [28] Xiao, H., Rasul, K., Vollgraf, R.: Fashion-mnist: a novel image dataset for benchmarking machine learning algorithms. arXiv preprint arXiv:1708.07747 (2017)
- [29] LeCun, Y., Cortes, C.: MNIST handwritten digit database. (2010)
- [30] Simonyan, K., Zisserman, A.: Very deep convolutional networks for large-scale image recognition. arXiv preprint arXiv:1409.1556 (2014)

- [31] Huang, G., Liu, Z., Van Der Maaten, L., Weinberger, K.Q.: Densely connected convolutional networks. In: Proceedings of the IEEE conference on computer vision and pattern recognition. (2017) 4700–4708
- [32] Szegedy, C., Liu, W., Jia, Y., Sermanet, P., Reed, S., Anguelov, D., Erhan, D., Vanhoucke, V., Rabinovich, A.: Going deeper with convolutions. In: Proceedings of the IEEE conference on computer vision and pattern recognition. (2015) 1–9
- [33] He, K., Zhang, X., Ren, S., Sun, J.: Deep residual learning for image recognition. In: Proceedings of the IEEE conference on computer vision and pattern recognition. (2016) 770–778
- [34] Cortes, C., Vapnik, V.: Support-vector networks. *Machine learning* **20**(3) (1995) 273–297
- [35] Moosavi-Dezfooli, S.M., Fawzi, A., Frossard, P.: Deepfool: a simple and accurate method to fool deep neural networks. In: Proceedings of the IEEE conference on computer vision and pattern recognition. (2016) 2574–2582
- [36] Szegedy, C., Zaremba, W., Sutskever, I., Bruna, J., Erhan, D., Goodfellow, I., Fergus, R.: Intriguing properties of neural networks. arXiv preprint arXiv:1312.6199 (2013)
- [37] Goodfellow, I.J., Shlens, J., Szegedy, C.: Explaining and harnessing adversarial examples. arXiv preprint arXiv:1412.6572 (2014)
- [38] Cheng, S., Dong, Y., Pang, T., Su, H., Zhu, J.: Improving black-box adversarial attacks with a transfer-based prior. In: Advances in Neural Information Processing Systems. (2019) 10932–10942
- [39] Akhtar, N., Jalwana, M.A., Bennamoun, M., Mian, A.: Label universal targeted attack. arXiv preprint arXiv:1905.11544 (2019)
- [40] Gao, Y., Xu, C., Wang, D., Chen, S., Ranasinghe, D.C., Nepal, S.: Strip: A defence against trojan attacks on deep neural networks. arXiv preprint arXiv:1902.06531 (2019)
- [41] Chen, H., Fu, C., Zhao, J., Koushanfar, F.: Deepinspect: A black-box trojan detection and mitigation framework for deep neural networks. In: Proceedings of the 28th International Joint Conference on Artificial Intelligence. AAAI Press. (2019) 4658–4664
- [42] Sedghi, M., Atia, G., Georgiopoulos, M.: Low-dimensional decomposition of manifolds in presence of outliers. In: 2019 IEEE 29th International Workshop on Machine Learning for Signal Processing (MLSP), IEEE (2019) 1–6